A new approach to calculate the water saturation in gas reservoirs with abnormal low resistivities in the Parnaiba Basin, Northeast Brazil.

Calonio, L. W.*, GIECAR's Lab-UFF; Freire, A. F. M., Professor-UFF; Ribeiro, L. F., GIECAR's Lab-UFF; Nobre, J. A., GIECAR's Lab-UFF; Lupinacci, W. M., Professor-UFF.

Abstract

The delta sandstones of the Poti Formation are the main reservoirs of Hawks Park, in the Parnaiba Basin. Despite being gas carries, these reservoirs have anomalously low resistivities, which directly impacts saturation calculations, leading to underestimations of their true potential. In order to contribute to the mitigation of this problem, a work flowchart is proposed for the characterization of the problem and correction of the resistivity curve, based on the case study of well PGN-5, seeking to obtain more reliable results for the evaluation of the reservoir. The methodology used is based on the integration of rock-logs-chemical data and the main inputs for this approach were: the cuttings samples, well logs, gamma-spectral data and analyzes through X-ray fluorescenceg. Thus, it was observed that the presence of clay minerals and pyrite are causes of low resistivities, even in the presence of gas-charged intervals, attested by density and neutron curves and pressure gradientes graph. This work proposes a correction factor for the resistivity curve in the anomalous zone, allowing a fresh evaluation of the well logs, leading to better calculations for net pay and gas saturation.

Introduction

The Parnaiba Basin is a paleozoic, intracratonic basin, producing natural gas, located in northeastern Brazil, which occupies an area of approximately 600,000 km^2. The sedimentary succession of the basin is divided into five Supersequences, which represent complete regressive transgressive cycles. The Mesodevonian-Eocarboniferous Supersequence holds the main oil systems in this basin. In this sense, the Poti Formation is the main reservoir in the most important production area of the basin today, called Hawks Park. The reservoir in focus presents the problem of anomalously low resistivities, because, for gas-charged intervals, high resistivity values are expected since the gaseous fluid is not conductive due to the low molecular density. This impacts directly on the saturation calculations and, consequently, leads to underestimations of net pay and requires special evaluations by the interpreter. Seaking to contribute to the mitigation of this problem in gas-charged reservoirs, a work flowchart is proposed for the reservoir characterization and correction of the resistivity curve (AT90), based on the case study of well PGN-5, in order to ain more realistic results to the evaluation of the reservoir. The methodology used is based on the integration of rock-log-chemical data, and the main inputs for this approach were: a) detailed description of the cuttings samples; b) basic suite of well logs; c) gamma-spectral data collected in cuttings samples and; d) chemical analysis through the of X-rays fluorecence (XRF). This work flowchart showed that the presence of clay minerals with a high cation exchange capacity (CEC) and diagenetic and framboidal pyrite are the causes of abnormal resistivities in the gas zone, having been generated a corrected resistivity curve with the creation of a correction factor.

Method

Searching to generate a detailed lithological profile, 64 cuttings samples from well PGN-5 were initially described in the reservoir interval (1336 / 1530 m). These descriptions were organized in the software SedLog. In parallel, a preliminary evaluation of the basic log suite was loaded out: Caliper, Gamma Ray (GR), Density (RHOZ), Neutron (NPOR), Resistivity (AT90), Sonic (DTCO) and Photoelectric Factor (PEFZ). The loading of these data and the lithological interpretation was performed using the software Trace. The gas-water contact in the well, once interpreted only by the AT90 curve (RT), is marked at 1369m (-1330 m). However, when the intersection of the RHOZ and NPOR curves in front of the reservoir was observed, the contact was setted up at 1418m (-1379 m) (Figure 1), despite the low resistivity values watched still in the gas carrier interval. The pressure gradient graph corroborated this analysis (Figure 2).

The rock data obtained with the cuttings samples show the presence of pyrite crystals and a highly clayeish reservoir, suggesting that these are the causes of this resistivity anomaly. To study these reservoir characteristics, two approaches were used:

- For the study of pyritization, the geochemical curves of the elements sulfide (S) and iron (Fe) were generated, obtained through XRF analysis. Since pyrite is an iron disulfide (FeS_2) these elements were taken as analogs of the mineral pyrite;
- The analysis of clay minerals was done using thorium (Th) and uranium (U) dispersion graphs, data obtained through a portable gamma-spectrometer on cuttings samples.

After characterizing the problem and detailing the Poti reservoir, the data were used to create a correction factor

for the AT90 curve. This new synthetic curve (RT_corrected) was plotted in the software Interactive Petrophysics (IP), along with the other data, and two evaluations were carried out with data on clay, porosity, water saturation and net pay.

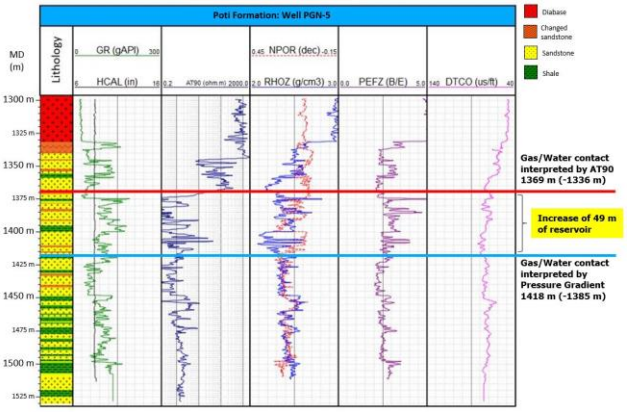

Figure 1 – *Image by Trace with lithological data (reinterpreted) and logs of the well PGN-5. Highlighted the interpretation of the gas-water contact by the pressure gradient graph compared to the contact given by the resistivity log (AT90). Source: Author.*

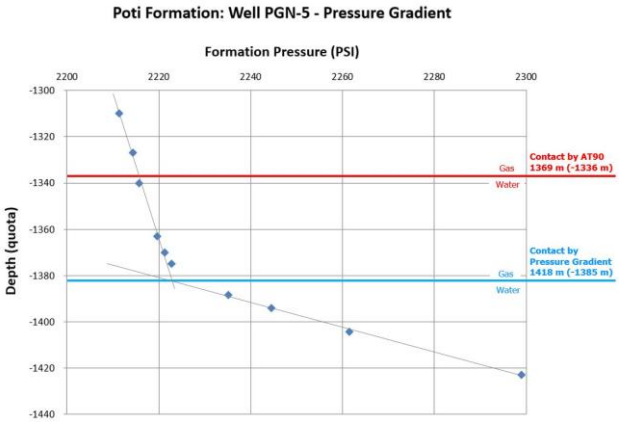

Figure 2 *– 'Depth x Pressure Gradient' graph used in the analysis of fluids and contacts from well PGN-5 in the reservoir interval (Poti Formation). Highlighted the gas-water contact depth (G/W) interpreted from the Resistivity (red line) and the Pressure Gradient (blue line). Source: Author.*

Results and Discussion

The comparison between the original lithological profile, present in the composite profile provided by BDEP / ANP, and the profile redescribed in this work, showed a much more clayish reservoir than the bulletin described (Figure 3).

Individualizing the type of mineral clay based only on the description of cuttings samples is not possible, but as some are more mandatory than others with regard to CEC and, consequently, for the AT90 curve, the gamma ray spectral data were plotted on a crossplot as proposed by Quirein (1982) and Klaja & Dudek (2016), whom propose to estimate which types of clay minerals are present based on a dispersion chart between Th (ppm) and K (%) (Figure 4).

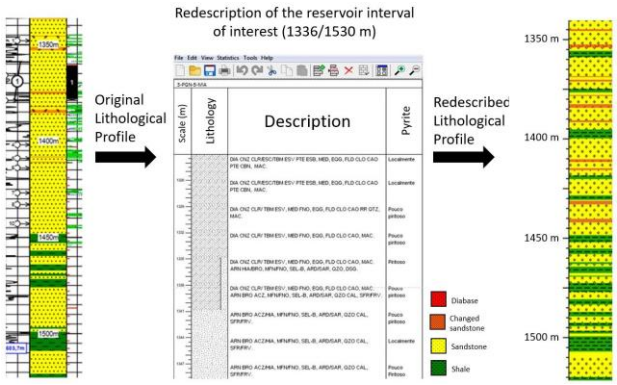

Figure 3 – *Profiles images before and after the reinterpretation of lithology from the descriptions of the cuttings samples. On the left the original lithological profile and on the right the reinterpreted profile. In the middle, an image from the software SedLog illustrating how the description data for the cuttings samples is plotted. Source: Author*

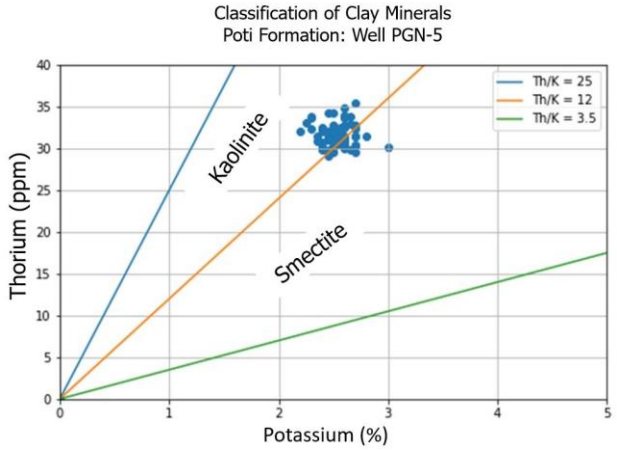

Figure 4 – *Scatter plot with Th and K data in Poti Formation, well PGN-5, to study the type of predominant clay minerals: kaolinite and smectite. Modified from Klaja & Dudek (2016).*

The graph showed the presence of kaolinite and smectite. Especially the presence of smectite, which is an expansive mineral and impacts the formation's resistivity, attenuating it due to the large amount of interstitial and conata water. Another important aspect, highlighted in the description of the cuttings samples, is that the abundant presence of pyrite, recognized as a conductive mineral. However, according to Clavier (1976), this mineral must be in percentages higher than 5-7% to affect the readings of the induction tool. Thus, in order to quantify a volume and apply it in the correction factor, Fe and S curves were generated derived from the XRF data, having been plotted with the other well logs (Figure 5).

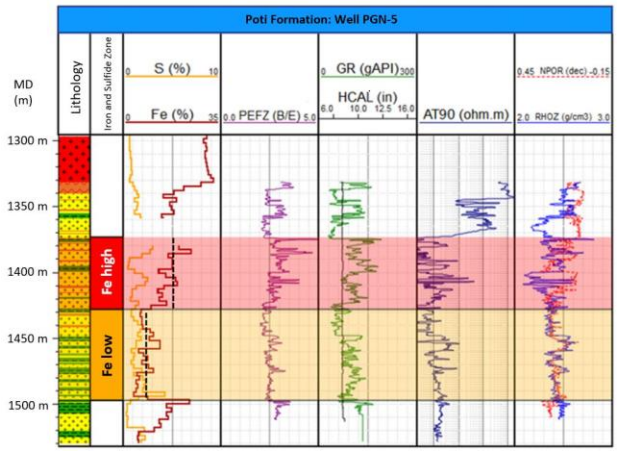

Figure 5 – *Lithological profile and logs of the well PGN-5 in the software Trace with emphasis, in red and orange, for the two sub-areas lined off according to the values of S and Fe. The dashed lines in black show average baselines for these contents. Source: Author.*

Two chemofacies were identified S-Fe_high and S-Fe_low. The S-Fe_high interval corresponds to the zone where the reservoir presents the biggest problems in resistivities. These high levels of Fe seem to come from the percolation of hydrothermal fluids associated with diabase intrusions present in Poti Fomation. It was possible to identify the presence of very silicified sandstones, indicating a potential metamorphism halo in the well, which coincides with the S-Fe_high zone. S is present in the shales, associated with organic matter, whose preservation is related to a reducing environment, ideal for the precipitation of sulfides such as pyrite.

From the XRF data, Fe and S percentages could be extracted and two graphs were also applied to quantify the volume of pyrite (Figure 6).

Although the large amount of pyrite observed in the cuttings samples, associated with the high levels of Fe and S present (Figure 7), the charts suggest that the pyrite would not be interfering with the AT90 values. A possible justification for this is that pyritization occurred not only in the sandstones of the reservoir, but also in the intragranular porosity of the shale at Poti Formation, in the form of microcrystalline framboidal pyrite grains, not connected to each other. So, there are two types of pyrite that occur in the reservoir and impact the readings: an euhedral pyrite, observed in the samples, with diagenetic origin; and another framboidal, microcrystalline, present in the shales (Figure 7). The latter is difficult to identify and seems to impact the tools in a different way, not being detected in the logs as expected.

Using the geochemical data, a correction factor for the AT90 log was empirically created to mitigate the impact of the conductivity given by the pyrite. The clayiness problem was overcome with the use of equations already applied usually for petrophysical evaluation. It was assumed that the original AT90 curve is "artificially" shifted to the low values due to an "increase in conductivity", given by the pyrite, which must be discounted so that the AT90 be corrected to the expected, in the case of a siliclastic reservoir gas-charged, as suggested by the Density and Neutron curves (Figure 1), beyond to the pressure gradient graph (Figure 2) as previously seen.

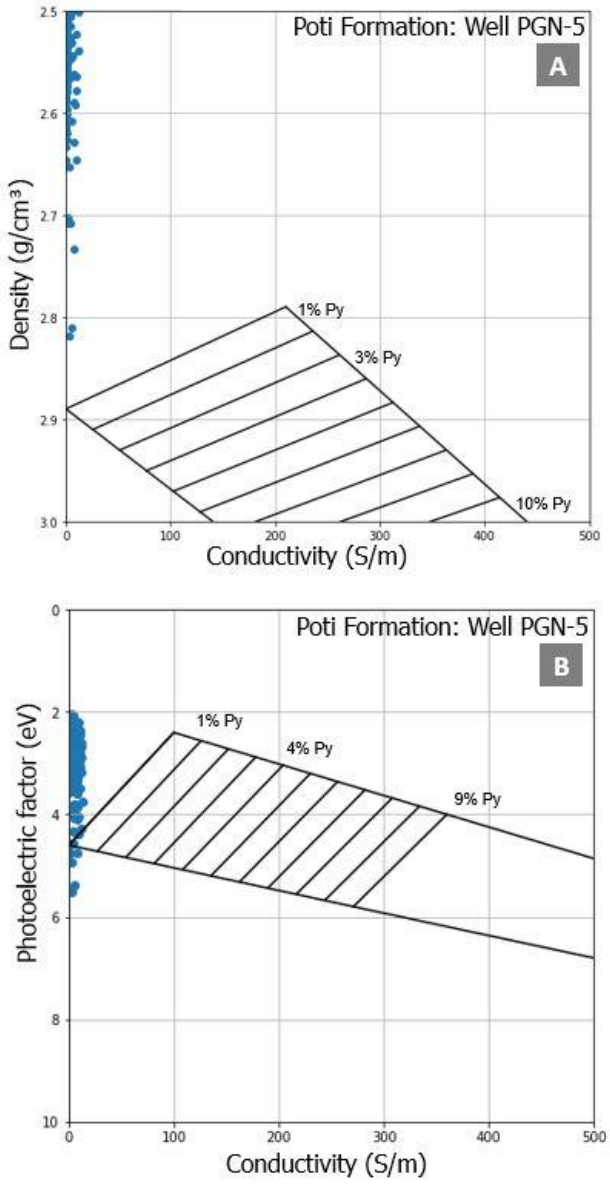

Figure 6 – *Charts to quantify pyrite volume in percentage; 7A (above): "Density x Conductivity" graph; 7B (below) 'PE x Conductivity' graph. Modified from Holmes et al. (2013).*

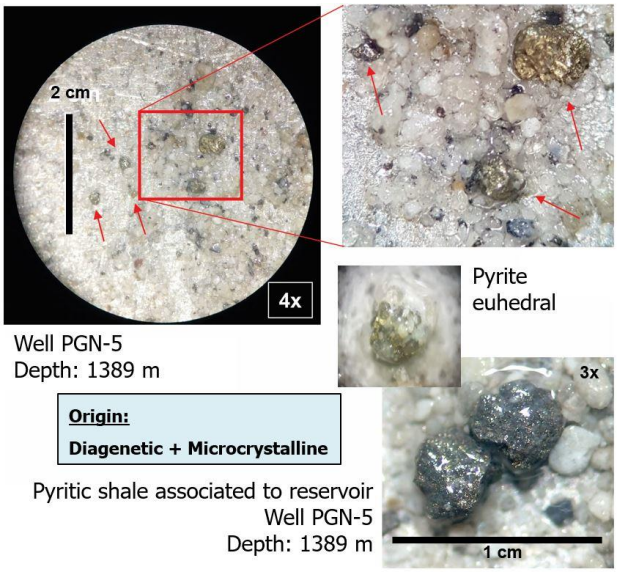

Figure 7 – *Picture of pyrite grains dispersed in the reservoir (sample depth 1389 m). In the shale sample there is framboidal pyrite and in the sandstone sample euhedral pyrites. Source: Author.*

Initially, two zones were individualized within the gas carrier range, Rtx and Rty (Figure 8).

The upper Rtx zone corresponds to a resistivity taken as a basis for values assumed to be regular, that is, less affected, with lower values of S-Fe. The lower Rty zone corresponds to na resistivity considered abnormally low, although it also refers to a gas-charged interval.

The saturation calculation demands correction, since the reservoir is underestimated when the input in the equation is the original AT90 curve. It is in this zone, where S and Fe has high values, that the correction factor was applied. This step was done in the software IP. Since the pyrite content and resistivity are inversely proportional variable, a relationship between them has been described:

$$\text{S-Fe normal X} \longrightarrow Rt_{normal}$$

$$\text{S-Fe high Y} \longrightarrow Fw*Rt_{affected}$$

Where,
(I) S-Fe normal X: Fe and S contents read at a point with "standard" resistivity;
(II) S-Fe high Y: Fe and S contents read at a point with affected resistivity;
(III) Rt_normal: Resistividade lida em um ponto onde não é afetada e apresenta valores "normais";
(IV) Rt_affected: resistivity read at a point where it is not affected and has "regular" values;
(V) Fw (conductivity fator): An empirical mediator between the variables, applied in a way to 'discount' the conductivity given by pyrite and to 'fix' the inverse relationship between the terms of the equation.

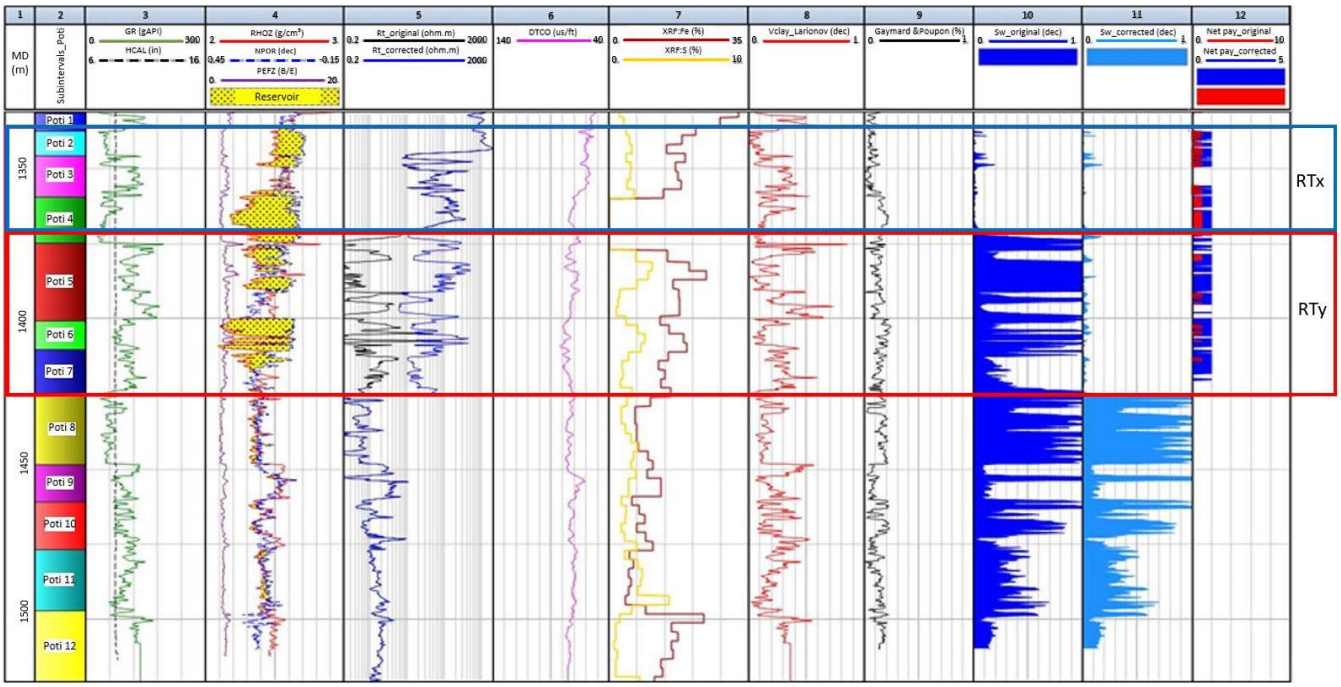

Figure 8 – *Figure 08: Image by IP with logs of well PGN-5. From left to right: Track 1: MD_Mesure Depth (m); Track 2: Subintervals_Poti; Track 3: GR: Gamma Ray (gAPI) / HCAL: Caliper (in); Track 4: RHOZ: Density (g/cm³) / NPOR: Neutron (dec) / PEFZ: Photoelectric factor (B/E); Track 5: Resistivity (ohm.m) where the original is the black curve and the corrected is the blue curve; Track 6: DTCO: Acustic (us/ft); Track 7: XRF:Fe% and XRF:S%; Track 8: Vclay_Larionov: Clayiness (%); Track 9: Gaymard & Poupon: Porosity (%); Track 10: SW_original: water saturation calculated from resistivity log (AT90) without correction (%); Track 11: SW_corrected: water saturation calculated from resistivity log (AT90) with correction (%); Track 12: Net pay_original (red) and Net pay_corrected (blue). Highlighted the Rtx (normal) and Rty (corrected) zones. Source: Author.*

The values (I) and (III) were extracted from the point 1435 m (Figure 1), chosen to present the expected resistivity for water saturation =100% in a sandstone below the gas zone. Its characteristics are: a) “clean” sandstone (GR = 59 API) inside the reservoir; b) water zone with normal resistivity (Rtwa <0.2 ohm.m); c) low values in S-Fe (Fe = 7%; S = 1.1%). Thus, we have:

$$Fw = \frac{(S/Fe_{high}) \times 0.2}{Rt_{affected} \times 0.157}$$

A second component of the factor was the sum of the 116.547 value obtained by subtracting the averages calculated to Rtx and Rty zones:

$$Rtx\_average - Rty\_average = 116.547$$

Fw and the value 116.547 were applied point to point on the AT90 curve, generating the corrected resistivity curve (RT_corrected) (Figure 8).

Two evaluations were made: one using the original AT90 and other applying the RT_corrected with the proposed correction, and the results could be compared between them (Figure 8). For the clay calculations, the equation proposed by Larionov (1969) was chosen for old rocks. For porosity, the Gaymard & Poupon (1970) equation was used because is indicate to minimize the gas effect. Saturation was estimated by Simandoux (1973), which is more adequate due to the clay character of the reservoir, since this equation considers other conductive materials in the rock fabrics besides the fluid. The results of saturation (tracks 10 and 11) and net pay (track 12) showing a reservoir gain when used at RT_corrected in the affected zone (zone Rty).

This result is supported and shown to be consistent with the crossover of the RHOZ and NPOR curves and the pressure gradient graph, through which the gas carrier interval was identified. It is worth noting that the saturation achieved with the corrected resistivity in the Rty zone was very similar to the saturation for the uncorrected resistivity in the Rtx zone. The porosity found varied from 6% to 18%, which is close to the value obtained in the data of the well folders, which gives an average porosity of 18%.

Conclusions

The Poti reservoir presents the problem of anomalously low resistivity. The well was redescribed, revealing a much more clayeish reservoir and the presence of pyrite, which causes the anomaly. Pyrite was interpreted as having a diagenetic and microcrystalline origin, replacing organic matter in the microporosity of clays, both related to the percolation of fluids induced by the Juro-Cretaceous magmatism of the basin. The clayiness was characterized as being predominantly composed of kaolinite and smectite, which show high CEC, observed through gamma-spectral data. The zone with the highest iron content presents the biggest problems in the behavior of the logs, especially in the AT90 curve and, with the data of S and Fe, a correction factor was proposed. This correction factor allowed the development of a corrected resistivity curve, used in the final evaluation of the reservoir, generating a significant reduction in water saturation and a remarkable net pay gain in the corrected zone. With this new calculation, the gas-water contact was reinterpreted, resulting in a increase of 49 meters of net pay. This workflow can be applied to reservoirs with similar characteristics, having been essential the integration of rock-logs-chemical data for the results and conclusions reached. To improve the correction factor and understand the impact of microcrystalline pyrite on the logs, this workflow should be extended to more wells.

Acknowledgments

The authors would like to thank to UFF’s laboratory GIECAR for the research infrastructure; to Petrobras for the financial resources used in this research; to ENEVA for donating the cuttings samples; to the other researchers who generated fundamental data for this work; and to the manager of the Parnaiba Project and my supervisor, Fernando Freire.

References

ARAÚJO L.M., TRIGÜIS J.A., CERQUEIRA J.R. & FREITAS L.C. DA S. 2000. The Atypical Permian Petroleum System of the Paraná Basin, Brazil. In: Mello M.R. & Katz B.J. (eds.) Petroleum Systems of South Atlantic Margins. AAPG Memoir, 73:377-402.

CALONIO, L. W. Influência de pirita e argilominerais nos cálculos de saturação da Fm. Poti, Bacia do Parnaíba: um estudo de caso no poço 3-PGN-5-MA. Dissertação (Mestrado em Geologia e Geofísica) – Instituto de Geociências, Geofísica, Universidade Federal Fluminende. Niterói – RJ, p. 160. 2020.

CAPUTO, Mário Vicente; IANNUZZI, R.; FONSECA, Vera Maria Medina. Bacias sedimentares brasileiras: Bacia do Parnaíba. Phoenix, v. 81, p. 1-6, 2005.

CUNHA, F.M.B. Evolução paleozóica CLAVIER, C. et al. Effect of pyrite on resistivity and other logging measurements. In: SPWLA 17th annual logging symposium. Society of Petrophysicists and Well-Log Analysts, 1976.

da bacia do Parnaíba e seu arcabouço tectônico.1986. 107p. Dissertação (Mestrado em Geologia) - Programa de Pós-graduação em Geologia, Instituto de Geociências, Universidade Federal do Rio de Janeiro, Rio de Janeiro.

DELLA FÁVERA, J.C. - 1980 - Reconhecimento de novas fácies e ambientes deposicionais da Bacia do Parnaíba. In: CONGRESSO BRASILEIRO DE GEOLOGIA,31., Camboriú, 1980. Resumos. Camboriú, SBG. p.357.

ELLIS, D. V., SINGER, J. M. Well Logging for Earth Scientists, Second Edition, Editora: Springer, Dordrecht, Holanda, 2008.

FERNANDES, R.F. 2011, Estudo da evolução termomecânica da Bacia do Parnaíba/ Regina Freitas Fernandes. – Rio de Janeiro:UFRJ/COPPE, 2011.

GÓES, A. M. A formação poti (carbonífero inferior) da Bacia do Parnaíba. 1995. 172 p. Tese (Doutorado) - Universidade de São Paulo, São Paulo, 1995.

GÓES, A. M. O.; FEIJÓ, F. J. Bacia do Parnaíba. Boletim de Geociências da Petrobras, Rio de Janeiro, v. 8, n. 1, p. 57-68, jan./mar. 1994.

HOLMES, Michael; HOLMES, Antony; HOLMES, Dominic. A Petrophysical Model to Quantify Pyrite Volumes and to Adjust Resistivity Response to Account for Pyrite Conductivity.2013.

KLAJA, Jolanta; DUDEK, Lidia. Geological interpretation of spectral gamma ray (SGR) logging in selected boreholes. Nafta-Gaz, v. 72, n. 1, p. 3-14, 2016.

LALANNE, Bruno JP et al. Impacts of petrophysical cut-offs in reservoir models. In: SPE Annual Technical Conference and Exhibition. Society of Petroleum Engineers, 2004.

MIRANDA, Frederico S. et al. Atypical igneous-sedimentary petroleum systems of the Parnaíba Basin, Brazil: seismic, well logs and cores. Geological Society, London, Special Publications, v. 472, n. 1, p. 341-360, 2018.

MIRANDA, F. S. Caracterização geológica da Formação Pimenteiras como potencial reservatório do tipo shale-gas (Devoniano da Bacia do Parnaíba). 2014. Tese de Doutorado. Dissertação (Mestrado em Geologia), Programa de Pós-graduação em Geologia, Instituto de Geociências, Universidade Federal do Rio de Janeiro, Rio de Janeiro.

RICKARD, D. Kinetics of pyrite formation by the H2S oxidation of iron(II) monosulfide in aqueous solution between 25 and 125ºC: the rate equation. Geochemica et Cosmochimica Acta, v. 61, p. 115-134. 1997.

RODRIGUES, R. A geoquímica orgânica na Bacia do Parnaíba. 1995. 226 p. Tese (Doutorado) – Universidade Federal do Rio Grande do Sul, Porto Alegre, 1995.

SAGEMAN, B.B. et al. A tale of shales: the relative roles of production, decomposition, and dilution in the accumulation of organic-rich strata, Middle–Upper Devonian, Appalachian basin. Chemical Geology, v.195, n.1, p.229-273, 2003.

SNEIDER, Robert M. Worldwide examples of low resistivity pay. 2003.

WILKIN, R. T., BARNES, H. L., BRANTLEY, S. L. The size distribuition of framboidal pyrite on modern sediments: Na indicator of redox conditions. Geochemica et Cosmochimica Acta, v. 60, n. 20, p. 3897-3912.